

Article

Self-Assembly of Discrete Metal Complexes in Aqueous Solution via Block Copolypeptide Amphiphiles

Keita Kuroiwa ^{1,*}, Yoshitaka Masaki ¹, Yuko Koga ¹ and Timothy J. Deming ²

¹ Department of Nanoscience, Faculty of Engineering, Sojo University, 4-22-1 Ikeda, Nishi-ku, Kumamoto 860-0082, Japan; E-Mails: 1114m07@gmail.com (Y.M.); 1214m03@gmail.com (Y.K.)

² Department of Bioengineering, University of California, Los Angeles, CA 90095, USA; E-Mail: demingt@seas.ucla.edu

* Author to whom correspondence should be addressed; E-Mail: keitak@nano.sojo-u.ac.jp; Tel./Fax: +81-96-326-3891.

Received: 11 December 2012; in revised form: 9 January 2013 / Accepted: 17 January 2013 / Published: 21 January 2013

Abstract: The integration of discrete metal complexes has been attracting significant interest due to the potential of these materials for soft metal-metal interactions and supramolecular assembly. Additionally, block copolypeptide amphiphiles have been investigated concerning their capacity for self-assembly into structures such as nanoparticles, nanosheets and nanofibers. In this study, we combined these two concepts by investigating the self-assembly of discrete metal complexes in aqueous solution using block copolypeptides. Normally, discrete metal complexes such as $[\text{Au}(\text{CN})_2]^-$, when molecularly dispersed in water, cannot interact with one another. Our results demonstrated, however, that the addition of block copolypeptide amphiphiles such as $\text{K}_{183}\text{L}_{19}$ to $[\text{Au}(\text{CN})_2]^-$ solutions induced one-dimensional integration of the discrete metal complex, resulting in photoluminescence originating from multinuclear complexes with metal-metal interactions. Transmission electron microscopy (TEM) showed a fibrous nanostructure with lengths and widths of approximately 100 and 20 nm, respectively, which grew to form advanced nanoarchitectures, including those resembling the weave patterns of *Waraji* (traditional Japanese straw sandals). This concept of combining block copolypeptide amphiphiles with discrete coordination compounds allows the design of flexible and functional supramolecular coordination systems in water.

Keywords: self-assembly; metal complexes; nanostructure; photoluminescence; metal-metal interaction; nanorod; block copolypeptides; amphiphiles

1. Introduction

There has, to date, been significant interest in the design and fabrication of low dimensional metal complexes, primarily because the electronic structures of such complexes are tunable via the formation of supramolecular architectures such as nanoparticles [1–19], nanocrystals [20–23] and nanowires [24–35]. The realization of dynamic correlations between molecular structures and supramolecular structures remains the most significant challenge in developing functional materials, which exhibit charge transfer, spin state crossover, photoluminescence and other useful properties. The luminescent properties of nanoscale metal complexes such as nanowires and nanocrystals are known to be especially sensitive to molecular structure, molecular conformation, metal-metal interactions and nanostructure [25,26,36,37]. The d^{10} gold(I) complexes, in particular, aggregate through d^{10} – d^{10} closed shell aurophilic bonding interactions, which determine both the supramolecular structures and luminescent properties of these materials [38,39].

As a result of its dynamic luminescence properties, $[\text{Au}(\text{CN})_2]^-$ has applications as a functional material within intelligent molecular systems. Both the wavelength and intensity of this luminescent emission can be tuned based on the aggregation of $[\text{Au}(\text{CN})_2]^-$ through Au-Au bonding interactions, although high concentrations (>10 mM) are required for luminescence at ambient temperatures [40–42]. At present, however, the relationships between molecular structure, metal-metal interactions and morphology at the nanoscale level are not thoroughly understood with regard to their effects on supramolecular structure, although simple polymers can lead to the polyelectrolyte with $[\text{Au}(\text{CN})_2]^-$ and self-assembly of polymeric $[\text{Au}(\text{CN})_2]^-$ [43]. The ability to tune the nanoscale morphology of these materials via molecular structure could lead to dramatic advances in the functionalities of systems incorporating metal complexes, and enable the dynamic hierarchical structural transformations, which lie at the very heart of bottom-up nanotechnology.

Diblock copolypeptide amphiphiles are synthetic materials with many features that make them of interest to those working in the field of protein engineering, in applications such as drug delivery systems and tissue engineering [44–50]. Their unique properties are due to the propensity of these amphiphiles to form double-walled vesicles or biocompatible fibrillar nanostructures based on the self-assembly of their hydrophilic and hydrophobic blocks. Moreover, the resulting hierarchical microstructures are suitable for integration with organic molecules, tissue cells and proteins. In addition, these copolypeptide structures can be used to tune various inorganic materials. They may, for example, be employed to modify the molecular structure, porosity and morphology of silica [51,52]. The inherent functional self-assembly abilities of these copolypeptide amphiphiles could potentially lead to their application not only as structural templates for inorganic compounds but also for the intelligent transformation of such inorganic materials involving dynamic tuning of the electronic state of the material.

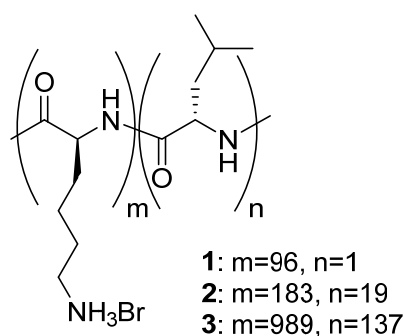
In this study, we focus on the dynamic structural transformation of $[\text{Au}(\text{CN})_2]^-$, achieved through the use of diblock copolypeptide amphiphiles having the general structural formula poly-L-Lysine-block-L-Leucine (K_mL_n). These amphiphiles are known to assemble into fibrillar structures, resulting in the formation of hydrogels and vesicles [52–55]. Our work investigated not only the morphological evolution associated with the aurophilic and polymeric interactions of the $[\text{Au}(\text{CN})_2]^-$, but also the hierarchical transformations of composite materials composed of combinations of the copolypeptides with the Au complex. The nature of the systematic assembly of these materials in solution is discussed, based on the results of spectroscopic and microscopic measurements.

2. Results and Discussion

2.1. Preparation of Copolypeptides

A number of diblock copolypeptide amphiphiles were synthesized according to procedures previously published in the literature [44,45]: K_{96}L_1 (**1**), $\text{K}_{183}\text{L}_{19}$ (**2**) and $\text{K}_{989}\text{L}_{137}$ (**3**) (Figure 1). All three copolypeptides exhibited low polydispersity values, ranging from 1.13 to 1.19, as measured by gel permeation chromatography (GPC) and ^1H NMR integration data for the lysine (Lys) moieties. When these copolypeptide amphiphiles were dissolved in water at concentrations above 1 wt%, hydrogels were obtained. This result indicates that all the synthesized copolymers formed fibrillar structures in aqueous solution as a result of self-assembly of the Lys and leucine (Leu) segments of the amphiphilic molecular structure.

Figure 1. Chemical structures of the diblock copolypeptide amphiphiles K_{96}L_1 (**1**), $\text{K}_{183}\text{L}_{19}$ (**2**) and $\text{K}_{989}\text{L}_{137}$ (**3**).

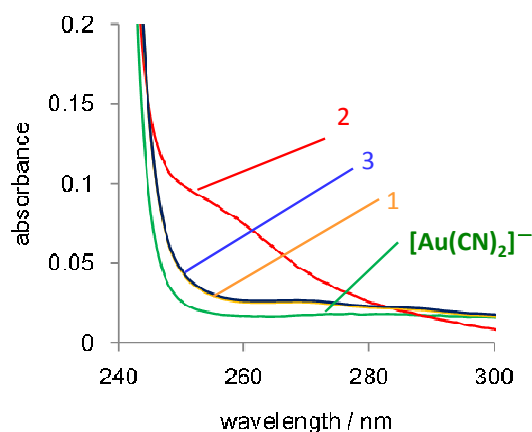


2.2. Spectroscopic Properties of Amphiphile/Metal Complex Composites

When $\text{K}[\text{Au}(\text{CN})_2]$ was added to aqueous solutions of the diblock copolypeptide amphiphiles at 1:1 molar ratios of $[\text{Au}(\text{CN})_2]$ to lysine unit, dispersion solutions were obtained. The associated aggregation and self-assembly of $[\text{Au}(\text{CN})_2]^-$ were investigated by UV-vis spectroscopy (Figure 2). The addition of 0.2 mM DI water solutions of $\text{K}[\text{Au}(\text{CN})_2]$ to diblock copolypeptide amphiphiles **1–3** resulted in the appearance of a new absorption shoulder in the region of 250 to 280 nm. Interestingly, the absorbance in this region was found to increase in the following order: **2**/ $[\text{Au}(\text{CN})_2]$ > **3**/ $[\text{Au}(\text{CN})_2]$ > **1**/ $[\text{Au}(\text{CN})_2]$. These observations suggest the oligomerization and/or polymerization of $[\text{Au}(\text{CN})_2]^-$

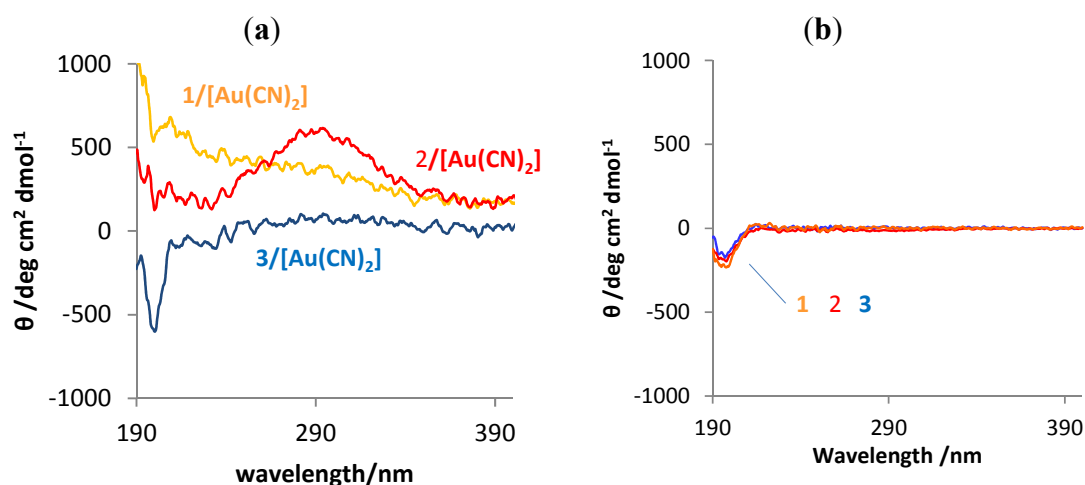
based on both electrostatic interactions with the positively charged side groups of the amphiphile Lys moieties and aurophilicity. Typically, when combining polylysine (without a Leu component) with $K[Au(CN)_2]$, an increase in the Lys to $K[Au(CN)_2]$ ratio results in a gradual increase in the absorbance of the shoulder at 250 to 300 nm [43]. It is therefore noteworthy that the copolypeptide amphiphiles in this work were synthesized to a degree of polymerization such that they were well suited to self-assembly and also were able to form structures, which promoted aurophilic interactions. In the case of these particular amphiphiles, it seems that not only their molecular structure and amphiphilic sequence, but also the degree to which they are polymerized has an effect on the aurophilic interactions of the metal complex composite.

Figure 2. UV-vis absorption spectra of composites **1**/ $[Au(CN)_2]^-$, **2**/ $[Au(CN)_2]^-$ and **3**/ $[Au(CN)_2]^-$ in deionized (DI) water. $[Au(CN)_2]^- = 0.2$ mM (Lys units: $K[Au(CN)_2] = 1:1$).



The circular dichroism (CD) spectra used to determine the conformations of the amino acids in water are presented in Figure 3a. In the composite mixtures, induced circular dichroism (ICD) appears in the absorbance region of 250 to 300 nm associated with $[Au(CN)_2]^-$, and the signal corresponding to such conformation as α -helix or β -sheet was not observed. The results indicate the assembly of $[Au(CN)_2]^-$ anions around the segments of the amphiphile backbone containing the cationic Lys, and a concurrent arrangement in the polymer conformation of random coil. In general, the CD spectra of diblock copolypeptide amphiphiles with Leu segment (greater than 20 residues) in DI water solutions at 293 K indicate an α -helix conformation due to hydrogen bonding interactions between the amino acids and hydrophobic interactions among the Leu segments [44,45]. On the other hand, **1**, **2**, and **3** cannot lead to the special secondary conformation due to much longer Lys segments (Figure 3b). Therefore, this result suggests that aurophilic and electrostatic interactions between the Lys segments and the $[Au(CN)_2]^-$, as well as hydrophobic interaction between the Leu segments, induced a random backbone.

Figure 3. (a) Circular dichroism (CD) spectra of **1**/[Au(CN)₂][−], **2**/[Au(CN)₂][−] and **3**/[Au(CN)₂][−] in DI water. [Au(CN)₂][−] = 0.2 mM. (Lys units:K[Au(CN)₂] = 1:1). (b) CD spectra of **1**, **2** and **3** in DI water ([Lys unit] = 0.2 mM).



It is well known that the specific conformations of protein molecules, such as α -helix, β -sheet or random coil, are closely associated with biological activity and play an important role in the functioning of the protein. Based on our general knowledge of polypeptides, the stabilization of a polypeptide's β -sheet structure using negatively charged metal complexes should be possible [43]. In the case of this study, however, interactions of the anionic metal complex with the Lys segments of the copolyptide amphiphiles induces conformational changes that transform the polymeric backbone to a random coil which in turn allows auropophilic interactions.

We also investigated the aggregation of [Au(CN)₂][−] and its auropophilic interactions by obtaining luminescence spectra of the amphiphile/[Au(CN)₂][−] composites. The excitation and emission spectra of composites **1–3**/[Au(CN)₂][−] (Lys units:K[Au(CN)₂] = 1:1) are shown in Figure 4. A 0.2 mM solution of [Au(CN)₂][−] in the absence of the copolyptide did not exhibit luminescence. In the case of a 2 mM [Au(CN)₂][−] solution, however, luminescence was observed at 343 nm (ex. 260 nm), a result which has previously been reported and attributed to the [Au(CN)₂][−] trimer [41,42]. The intensity of the luminescence increased following the addition of amphiphiles **1** to **3**. Amphiphile **2** in particular resulted in a dramatic increase in luminescence intensity (Figure 5). The effect of varying the stoichiometric ratio of the composite solution was also investigated, based on the addition of **2** to a 0.2 mM [Au(CN)₂][−] solution in deionized (DI) water. The addition of **2** (0.2 to 1 molar equivalents of the Lys unit) to K[Au(CN)₂] induced a sigmoidal increase of the emission intensity, as well as a red shift of the emission band to 465 nm (ex. 271 nm) (Figure 6). Further addition of **2** (1 to 10 molar equivalents of the Lys unit) led to a decrease in the emission intensity with a slight blue shift of the emission band to 456 nm (Figure 5). It has been reported that the luminescence band resulting from the Au–Au bond may be attributed to polynuclear [Au(CN)₂][−]_n excimers and exciplexes [41,42]. Furthermore, the red-shifted emission band (seen upon adding 0.2 to 1 molar equivalents Lys) indicates longer polynuclear Au complexes than were present in the initial solution of the complex, whereas the blue shift (at 1 to 10 molar equivalents Lys) suggests a decrease in polynuclear species due to disordered Au–Au interactions (Figure 5). In contrast, amphiphile **1** (which had a lower extent

of polymerization than **2**) and amphiphile **3** (which had a greater extent of polymerization than **2**) only caused slight increases in luminescent intensity. These results indicate that electrostatic and van der Waals interactions with the amphiphiles play a significant role in the luminescence resulting from the Au-Au interactions. Based on these studies concerning the self-assembly of $[\text{Au}(\text{CN})_2]^-$ with the diblock copolypeptide amphiphiles, we conclude that the aurophilic interaction is readily controlled via both the concentration of the metal complex in solution and the molar ratio between the peptide and the complex.

Figure 4. Fluorescence spectra of **1**/ $[\text{Au}(\text{CN})_2]^-$, **2**/ $[\text{Au}(\text{CN})_2]^-$ and **3**/ $[\text{Au}(\text{CN})_2]^-$ in DI water. $[\text{Au}(\text{CN})_2]^- = 0.2 \text{ mM}$. (Lys units:K $[\text{Au}(\text{CN})_2]^- = 1:1$).

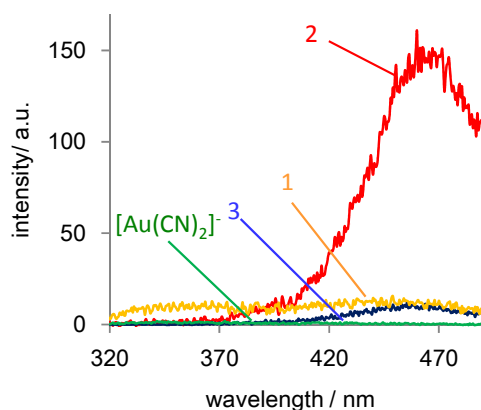


Figure 5. (a,b) Variations in the fluorescent intensity of **2**/ $[\text{Au}(\text{CN})_2]^-$ with changes in the lysine: $[\text{Au}(\text{CN})_2]^-$ molar ratio (a: 0–10, b: 0–2) in DI water. (c) Variations in the fluorescence wavelength of **2**/ $[\text{Au}(\text{CN})_2]^-$ with changes in the lysine: $[\text{Au}(\text{CN})_2]^-$ molar ratio in DI water. $[\text{Au}(\text{CN})_2]^- = 0.2 \text{ mM}$.

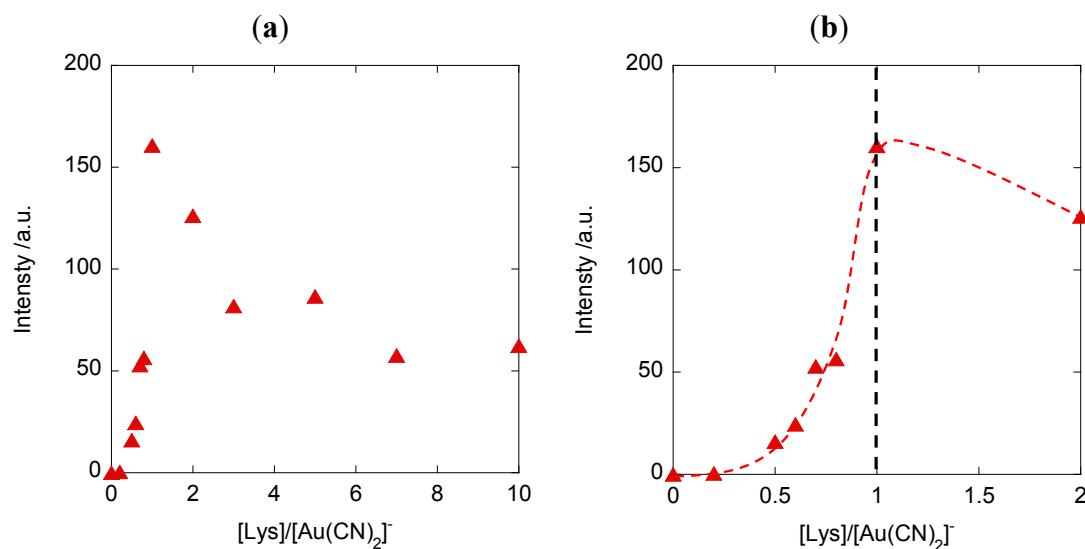


Figure 5. Cont.

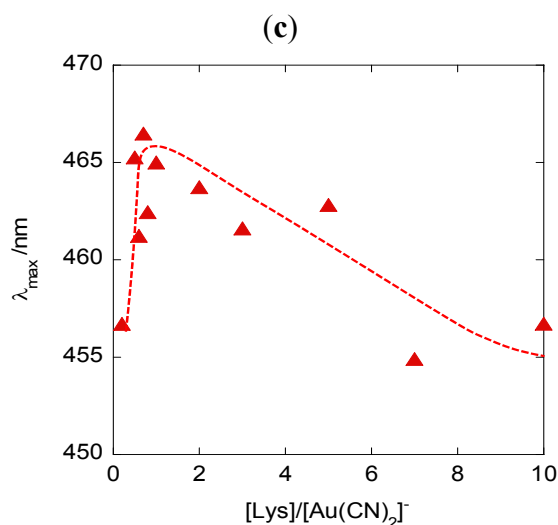
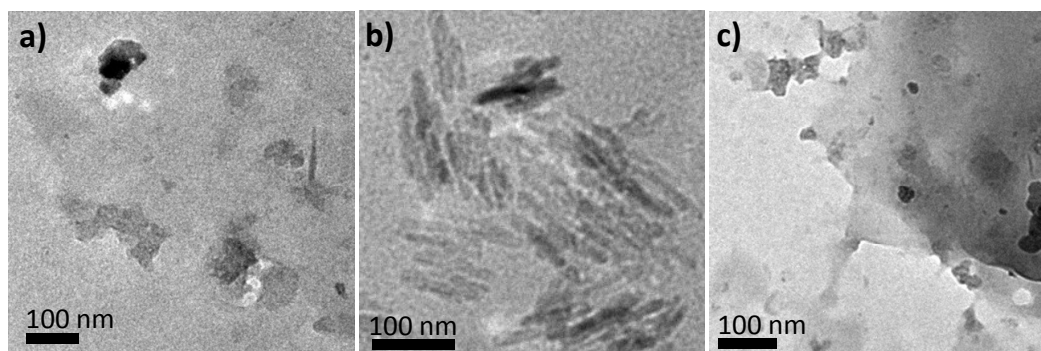


Figure 6. Transmission electron micrographs of samples prepared from (a) **1**/[Au(CN)₂]⁻, (b) **2**/[Au(CN)₂]⁻ and (c) **3**/[Au(CN)₂]⁻ in DI water solutions. Samples are not stained.

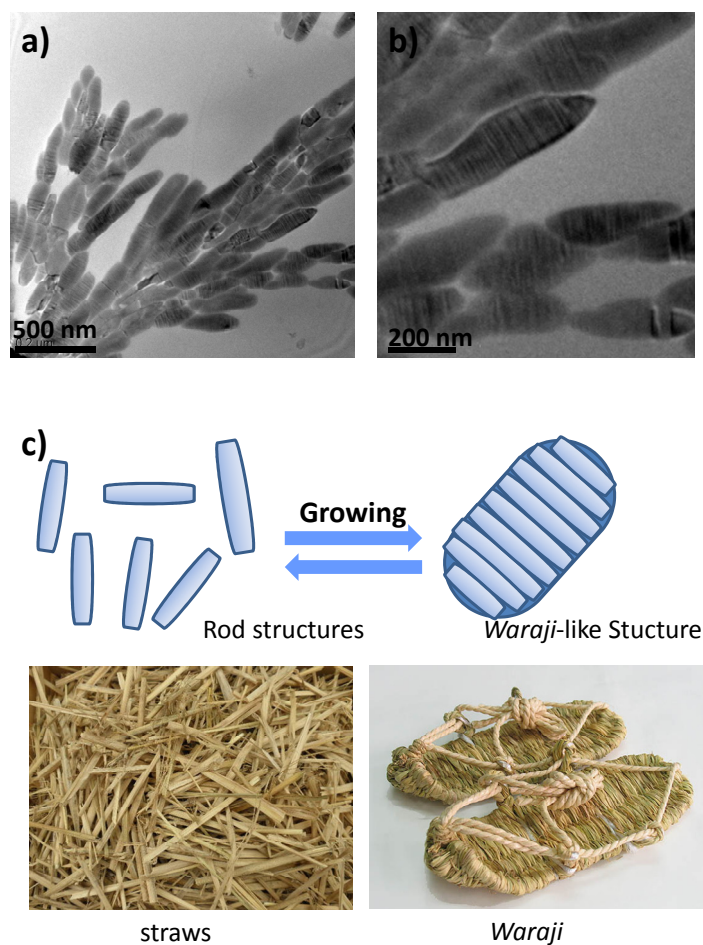


2.3. Morphological Characterization of Amphiphile/Metal Complex Composites

To examine the detailed nanostructures of the amphiphile/[Au(CN)₂]⁻ complexes, transmission electron micrographs of DI water solutions of **1**/[Au(CN)₂]⁻, **2**/[Au(CN)₂]⁻ and **3**/[Au(CN)₂]⁻ were acquired (Figure 6). These samples were not stained, and the dark regions are ascribed to Au present in the composites. Both **1**/[Au(CN)₂]⁻ (Figure 6a) and **3**/[Au(CN)₂]⁻ (Figure 6c) display indefinite structures or sheet structures several hundred nanometers long. Although it is possible that both the irregular and layered structures were formed during sample preparation, as a result of evaporation on the carbon-coated Cu mesh, it is more likely that these nanostructures were randomly generated as a consequence of partial dissociation of polynuclear [Au(CN)₂]⁻_n complexes into shorter structures in association with random-coiled copolypeptides. Surprisingly, **2**/[Au(CN)₂]⁻ (Figure 6b) exhibited numerous rectangular nanorods (length: 90–150 nm, width: 15–30 nm) together with some nanocrystals. These nanostructures are more developed than those of **1** and **3** and it is clear that the regular supramolecular structure resulting from **2** is due to the self-assembly of [Au(CN)₂]⁻ in conjunction with the copolypeptide amphiphile. These results are consistent with the polynuclear behavior deduced from UV-vis, CD and luminescence spectral data.

When one molar equivalent of a 5 mM DI water solution of $\text{K}[\text{Au}(\text{CN})_2]$ was added to a 5 mM (in terms of Lys units) DI water solution of **2**, a colloidal dispersion was obtained. Samples prepared from this solution displayed a nanostructure vaguely similar to the weave pattern of the traditional Japanese *Waraji* (straw sandals), with regular sections consisting of assembled nanorods 15–30 nm in length (Figure 7). This *Waraji*-like nanostructure presumably formed as the result of self-assembly of nanorods composed of the metal complex/amphiphile composite. It is known that diblock copolymer with a hydrophilic part and a hydrophobic part form one-directionally stacked lamellar structures due to the nucleation of lamellar layers, and the lamellar layers were anisotropically grown in the nanostructures [53,54]. Diblock copolypeptide amphiphiles and metal complexes therefore are capable of interacting not only at the molecular level but also at the subnanometer scale to form hierarchical structures, a phenomenon similar to the manner in which the quaternary structures of proteins are formed.

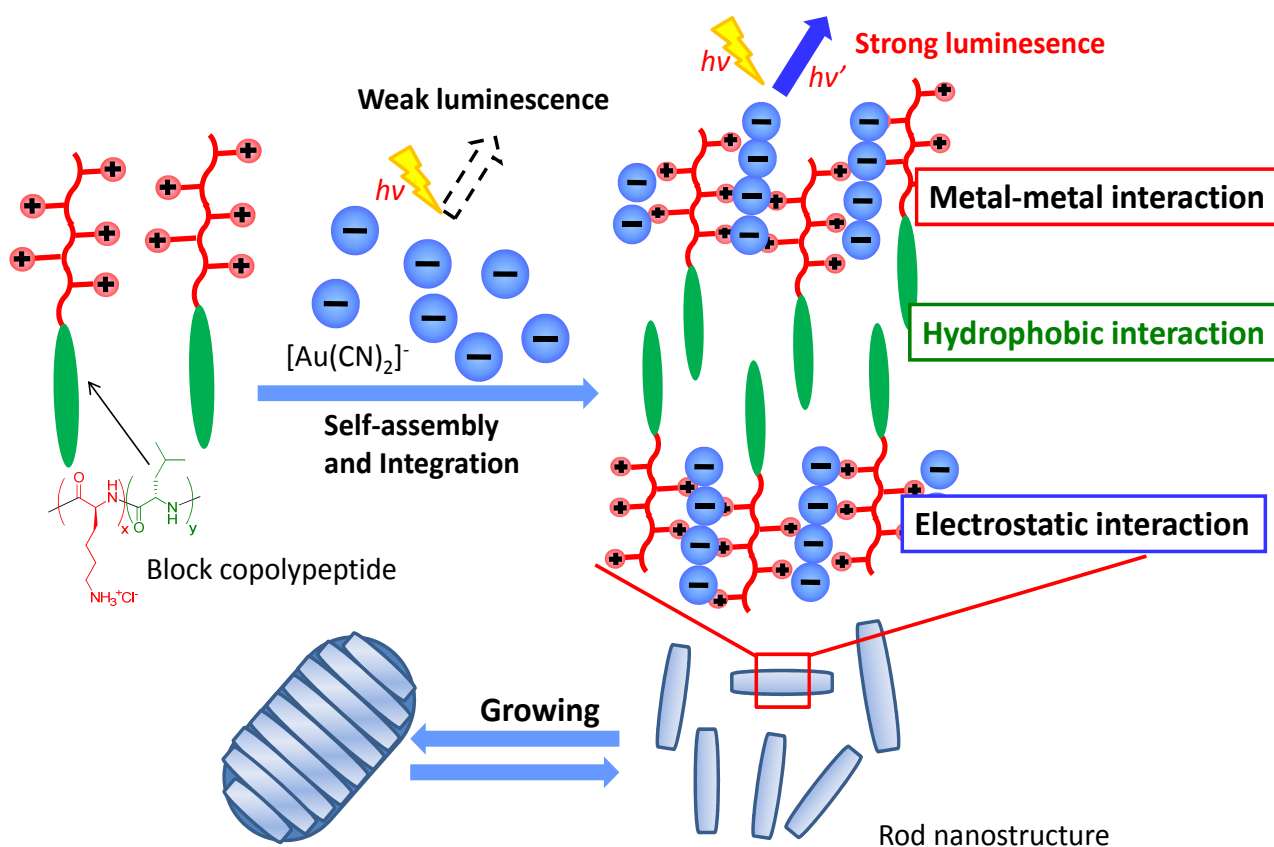
Figure 7. (a) Transmission electron micrograph of samples prepared from $\mathbf{2}/[\text{Au}(\text{CN})_2]^-$ ($[\text{Au}(\text{CN})_2] = 5 \text{ mM}$ (Lys units: $\text{K}[\text{Au}(\text{CN})_2] = 1:1$)). (b) Transmission electron micrographs of samples prepared from $\mathbf{2}/[\text{Au}(\text{CN})_2]^-$ ($[\text{Au}(\text{CN})_2] = 5 \text{ mM}$ (Lys units: $\text{K}[\text{Au}(\text{CN})_2] = 1:1$)) at higher magnification than micrograph (a). (c) Schematic illustration of rod structure to *Waraji* nanostructures comparing the Japanese *Waraji* (straw sandal) photographs.



The results from our spectroscopic and morphological investigations provide detailed information regarding the nature of the composites self-assembled from diblock copolypeptide amphiphiles and the

metal complex, as illustrated in Figure 8. The data from UV-vis absorption and luminescence intensity analyses show that the amphiphile/ $[\text{Au}(\text{CN})_2]^-$ complexes include polynuclear $[\text{Au}(\text{CN})_2]_n$ species which undergo Au-Au bonding interactions. In addition, based on the results obtained when using a molar ratio between the Lys component of the polypeptide and $[\text{Au}(\text{CN})_2]^-$ of 1:1, the electrostatic interactions between the Lys segments and the anionic $[\text{Au}(\text{CN})_2]^-$ play a significant role in enabling the aurophilic interactions. In particular, the observations concerning aurophilic interactions indicate that $[\text{Au}(\text{CN})_2]^-$ forms ordered arrays together with the copolypeptide amphiphiles. High-resolution transmission electron microscopy (HR-TEM) observations show molecular-scale rod structures forming complex *Waraji*-like structures, depending on the concentration of the composite solution. It is therefore evident that the amphiphile is capable of inducing interesting alignment structures in aqueous solutions of the metal complex.

Figure 8. Schematic illustration of self-assembly of copolypeptide amphiphiles/Au complexes to develop the functional nanostructure.



3. Experimental Section

3.1. Materials and Instrumentation

Tetrahydrofuran (THF) and hexane were dried by purging with nitrogen. $\text{Co}(\text{PMe}_3)_4$ was prepared according to procedures previously published in the literature. All chemicals were purchased from commercial suppliers (Tokyo Kasei, Wako Co., Ltd., Kanto Chemical Co., Ltd., and Sigma-Aldrich Chemical Co.) and used without further purification unless otherwise noted. Fourier Transform Infrared Spectroscopy (FTIR) measurements were obtained on a Spectrum 65 FT-IR (PerkinElmer,

Inc.). ^1H nuclear magnetic resonance (NMR) spectra were acquired using an ESC 400 (JEOL Ltd.). Gel permeation chromatography/light scattering (GPC/LS) was performed at 333 K using a Waters high performance liquid chromatography (HPLC) system incorporating a 410 differential refractometer detector and a 1515 pump/controller. Separations were achieved using 10^5 , 10^4 and 10^3 Å Phenomenex Phenogel 5 μm columns with 0.1 M LiBr in DMF as the eluent and sample concentrations of 5 mg/mL. Pyrogen-free deionized water (DI) was obtained from Advantec RFD240NA and RFU655DA purification units. UV-vis spectra and fluorescence spectra were obtained on RF-2500PC and RF-5300PC spectrophotometers, respectively (Shimadzu Co., Ltd.). Transmission electron microscopy was performed using a Tecnai G² F20 (FEI Co.) operating at 200 kV. Transmission electron microscope samples were prepared by transferring the surface layers of gels or solutions to carbon-coated TEM grids.

3.2. General Polypeptide Synthesis

All diblock copolypeptide amphiphiles were synthesized using $\text{Co}(\text{PMe}_3)_4$ as the initiator, according to the literature procedures[44,45]. Protected diblock copolypeptide amphiphiles were first purified and then characterized using GPC/LS and FTIR. The protecting groups on the N_ϵ -benzyloxycarbonyl-L-lysine moieties were removed to produce residual L-lysine·HBr in the copolypeptides by the addition of 33 wt% HBr in acetic acid to a solution of copolymer in trifluoroacetic acid (TFA) at 273 K, followed by stirring for 1 h. All deprotected copolymers were dissolved in and then dialyzed exhaustively against non-pyrogenic DI water. Lyophilization of these solutions gave the copolymers as white powders. Chain lengths of Km segments were determined using GPC, with measured polydispersities (M_w/M_n) ranging from 1.13 to 1.19. ^1H NMR in deuterium oxide (D_2O) indicated over 99.9% removal of the benzyloxycarbonyl groups from the lysine residues.

3.3. General Preparation of Copolypeptide/ $[\text{Au}(\text{CN})_2]^-$ Composites

Ternary composites were prepared by mixing DI water solutions of $\text{K}[\text{Au}(\text{CN})_2]$ (0.2 mM, 1 mL) with DI water solutions of diblock copolypeptide amphiphiles **1** to **3** (0.2 mM, 1 mL) at room temperature. All composite solutions prepared in this manner were stable in oxygen-free DI water for a period of one month, although pure $\text{K}[\text{Au}(\text{CN})_2]$ in DI water was unstable in air and decomposed with the formation of both oxidation and hydrolysis products, with a concurrent loss of photoluminescence. The observed stabilization induced on adding the amphiphiles indicates that aggregation of the composites subsequent to the copolypeptides addition prevents $[\text{Au}(\text{CN})_2]^-$ from reacting with oxygen (see Section 2.3).

4. Conclusions

We have demonstrated the formation of diblock copolypeptide amphiphile/metal complex composites, with significant variation in nanostructure depending on the structure of the copolypeptide. The formation of composite materials produced by combining these amphiphiles with the metal complex demonstrates that it is possible to control the complex's metal-metal interactions and produce one-dimensional structures such as rods, as well as more complex architectures such as the

Waraji structure. The technique of combination of amphiphilic molecules and discrete coordination compounds [55,56] makes it possible to design flexible, reversible, and signal-responsive supramolecular coordination systems. This general concept of a biopolymer composite could be expanded to include other useful compounds and should provide valuable information leading to further advances in the field of coordination materials and biopolymer nanochemistry.

Acknowledgments

This work was financially supported in part by a Grant-in-Aid for Young Scientists (A) (No. 24685019), and a Grant-in-Aid from the Global COE Program “Science for Future Molecular Systems” by the Ministry of Education, Culture, Sports, Science and Technology of Japan and JST CREST. Seiji Shinkai and Shin-ichi Tamaru at Sojo University are thanked for their assistance with gel permeation chromatography/light scattering (GPC/LS). K. K. was also supported by the Ministry of Education, Culture, Sports, Science and Technology, JAPAN (S0801085).

References

1. Suh, J.; Shim, H.; Shin, S. Coordinatively Polymerized Bilayer Membranes Prepared in Formamide. *Langmuir* **1996**, *12*, 2323–2324.
2. Moulik, S.P.; De, G.C.; Panda, A.K.; Bhowmik, B.B.; Das, A.R. Dispersed Molecular Aggregates. 1. Synthesis and Characterization of Nanoparticles of $\text{Cu}_2[\text{Fe}(\text{CN})_6]$ in $\text{H}_2\text{O}/\text{AOT}/n\text{-Heptane}$ Water-in-Oil Microemulsion Media. *Langmuir* **1999**, *15*, 8361–8367.
3. Vaucher, S.; Li, M.; Mann, S. Synthesis of Prussian Blue Nanoparticles and Nanocrystal Superlattices in Reverse Microemulsions. *Angew. Chem. Int. Ed.* **2000**, *39*, 1793–1796.
4. Vaucher, S.; Fielden, J.; Li, M.; Dujardin, E.; Mann, S. Molecule-Based Magnetic Nanoparticles: Synthesis of Cobalt Hexacyanoferrate, Cobalt Pentacyanonitrosylferrate, and Chromium Hexacyanochromate Coordination Polymers in Water-in-Oil Microemulsions. *Nano Lett.* **2002**, *2*, 225–229.
5. Uemura, T.; Kitagawa, S. Prussian Blue Nanoparticles Protected by Poly(vinylpyrrolidone). *J. Am. Chem. Soc.* **2003**, *125*, 7814–7815.
6. Uemura, T.; Ohba, M.; Kitagawa, S. Size and Surface Effects of Prussian Blue Nanoparticles Protected by Organic Polymers. *Inorg. Chem.* **2004**, *43*, 7339–7345.
7. Hu, M.; Furukawa, S.; Ohtani, R.; Sukegawa, H.; Nemoto, Y.; Reboul, J.; Kitagawa, S.; Yamauchi, Y. Synthesis of Prussian Blue Nanoparticles with a Hollow Interior by Controlled Chemical Etching. *Angew. Chem. Int. Ed.* **2012**, *51*, 984–988.
8. Domínguez-Vera, J.M.; Colacio, E. Nanoparticles of Prussian Blue Ferritin: A New Route for Obtaining Nanomaterials. *Inorg. Chem.* **2003**, *42*, 6983–6985.
9. Yamada, M.; Arai, M.; Kurihara, M.; Sakamoto, M.; Miyake, M. Synthesis and Isolation of Cobalt Hexacyanoferrate/Chromate Metal Coordination Nanopolymers Stabilized by Alkylamino Ligand with Metal Elemental Control. *J. Am. Chem. Soc.* **2004**, *126*, 9482–9483.
10. Fiorito, P.A.; Gonçalves, V.R.; Ponzio, E.A.; de Torresi, S.I.C. Synthesis, characterization and immobilization of Prussian blue nanoparticles. A potential tool for biosensing devices. *Chem. Commun.* **2005**, 366–368.

11. Taguchi, M.; Yamada, K.; Suzuki, K.; Sato, O.; Einaga, Y. Photoswitchable Magnetic Nanoparticles of Prussian Blue with Amphiphilic Azobenzene. *Chem. Mater.* **2005**, *17*, 4554–4559.
12. Sun, X.; Dong, S.; Wang, E. Coordination-Induced Formation of Submicrometer-Scale, Monodisperse, Spherical Colloids of Organic-Inorganic Hybrid Materials at Room Temperature. *J. Am. Chem. Soc.* **2005**, *127*, 13102–13103.
13. Park, K.H.; Jang, K.; Son, S.U.; Sweigart, D.A. Self-Supported Organometallic Rhodium Quinonoid Nanocatalysts for Stereoselective Polymerization of Phenylacetylene. *J. Am. Chem. Soc.* **2006**, *128*, 8740–8741.
14. Oh, M.; Mirkin, C.A. Chemically tailorable colloidal particles from infinite coordination polymers. *Nature* **2005**, *438*, 651–654.
15. Maeda, H.; Hasegawa, M.; Hashimoto, T.; Kakimoto, T.; Nishio, S.; Nakanishi, T. Nanoscale Spherical Architectures Fabricated by Metal Coordination of Multiple Dipyrin Moieties. *J. Am. Chem. Soc.* **2006**, *128*, 10024–10025.
16. Imaz, I.; Maspoch, D.; Rodríguez-Blanco, C.; Pérez-Falcón, J.M.; Campo, J.; Ruiz-Molina, D. Valence-Tautomeric Metal–Organic Nanoparticles. *Angew. Chem. Int. Ed.* **2008**, *47*, 1857–1860.
17. Coronado, E.; Galán-Mascarós, J.R.; Monrabal-Capilla, M.; García-Martínez, J.; Pardo-Ibañez P. Bistable Spin-Crossover Nanoparticles Showing Magnetic Thermal Hysteresis near Room Temperature. *Adv. Mater.* **2007**, *19*, 1359–1361.
18. Boldog, I.; Gaspar, A.B.; Martínez, V.; Pardo-Ibañez, P.; Ksenofontov, V.; Bhattacharjee, A.; Gütllich, P.; Real, J.A. Spin-Crossover Nanocrystals with Magnetic, Optical, and Structural Bistability near Room Temperature. *Angew. Chem. Int. Ed.* **2008**, *47*, 6433–6437.
19. Liang, G.; Xu, J.; Wang, X. Synthesis and Characterization of Organometallic Coordination Polymer Nanoshells of Prussian Blue Using Miniemulsion Periphery Polymerization (MEPP). *J. Am. Chem. Soc.* **2009**, *131*, 5378–5379.
20. Rieter, W.J.; Taylor, K.M.L.; An, H.; Lin, W.; Lin, W. Nanoscale Metal–Organic Frameworks as Potential Multimodal Contrast Enhancing Agents. *J. Am. Chem. Soc.* **2006**, *128*, 9024–9025.
21. Taylor, K.M.L.; Rieter, W.J.; Lin, W. Manganese-Based Nanoscale Metal–Organic Frameworks for Magnetic Resonance Imaging. *J. Am. Chem. Soc.* **2008**, *130*, 14358–14359.
22. Jung, S.; Oh, M. Monitoring Shape Transformation from Nanowires to Nanocubes and Size-Controlled Formation of Coordination Polymer Particles. *Angew. Chem. Int. Ed.* **2008**, *47*, 2049–2051.
23. Rieter, W.J.; Pott, K.M.; Taylor, K.M.L.; Lin, W. Nanoscale Coordination Polymers for Platinum-Based Anticancer Drug Delivery. *J. Am. Chem. Soc.* **2008**, *130*, 11584–11585.
24. Suh, J.; Lee, K.J.; Bae, G.; Kwon, O.-B.; Oh, S. Coordinatively Polymerized Bilayer Membranes Prepared by Metal Complexation of an Amphiphilic *o,o'*-Dihydroxyazobenzene Derivative. *Langmuir* **1995**, *11*, 2626–2632.
25. Breimi, J.; Brovelli, D.; Caseri, W.; Hähner, G.; Smith, P.; Tervoort, T. From Vauquelin's and Magnus' Salts to Gels, Uniaxially Oriented Films, and Fibers: Synthesis, Characterization, and Properties of Tetrakis(1-aminoalkane)metal(II) Tetrachlorometalates(II). *Chem. Mater.* **1999**, *11*, 977–994.
26. Grate, J.W.; Moore, L.K.; Janzen, D.E.; Veltkamp, D.J.; Kaganove, S.; Drew, S.M.; Mann, K.R. Steplike Response Behavior of a New Vapochromic Platinum Complex Observed with

- Simultaneous Acoustic Wave Sensor and Optical Reflectance Measurements. *Chem. Mater.* **2002**, *14*, 1058–1066.
27. Kurth, D.G.; Severin, N.; Rabe, J.P. Perfectly Straight Nanostructures of Metallosupramolecular Coordination- Polyelectrolyte Amphiphile Complexes on Graphite. *Angew. Chem. Int. Ed.* **2002**, *41*, 3681–3683.
28. Roubeau, O.; Colin, A.; Schmitt, V.; Clérac, R. Thermoreversible Gels as Magneto-Optical Switches. *Angew. Chem. Int. Ed.* **2004**, *43*, 3283–3286.
29. Kimizuka, N. Self-assembly of supramolecular nanofibers. *Adv. Polym. Sci.* **2008**, *219*, 1–26.
30. Kimizuka, N.; Oda, N.; Kunitake, T. Supramolecular assemblies comprised of one-dimensional mixed valence platinum complex and anionic amphiphiles in organic media. *Chem. Lett.* **1998**, *27*, 695–696.
31. Kuroiwa, K.; Shibata, T.; Takada, A.; Nemoto, N.; Kimizuka, N. Heat-set gel-like networks of lipophilic Co^{II} triazole complexes in organic media and their thermochromic structural transitions. *J. Am. Chem. Soc.* **2004**, *126*, 2016–2021.
32. Kuroiwa, K.; Kimizuka, N. Coordination structure changes of linear cobalt(II) triazole complexes induced by binding of long-chained alcohols: Adaptive molecular clefts, *Chem. Lett.* **2008**, *37*, 192–193.
33. Kuroiwa, K.; Kimizuka, N. Electrochemically controlled self-assembly of lipophilic Fe^{II} 1,2,4-triazole complexes in organic media. *Chem. Lett.* **2010**, *39*, 790–791.
34. Kuroiwa, K.; Shibata, T.; Sasaki, S.; Ohba, M.; Takahara, A.; Kunitake, T.; Kimizuka, N. Supramolecular control of spin crossover phenomena in lipophilic Fe^{II} 1,2,4-triazole complexes. *J. Polym. Sci. A Polym. Chem.* **2006**, *44*, 5192–5202.
35. Kuroiwa, K.; Kikuchi, H.; Kimizuka, N. Spin crossover characteristics of nanofibrous Fe^{II}-1,2,4-triazole complexes in liquid crystals. *Chem. Commun.* **2010**, *46*, 1229–1231.
36. Yam, V.W.-W.; Cheng, E.C.-C. Highlights on the recent advances in gold chemistry—A photophysical perspective. *Chem. Soc. Rev.* **2008**, *37*, 1806–1813.
37. Wong, K.M.-C.; Yam, V.W.-W. Self-Assembly of Luminescent Alkynylplatinum(II) Terpyridyl Complexes: Modulation of Photophysical Properties through Aggregation Behavior. *Acc. Chem. Res.* **2011**, *44*, 424–434.
38. Kishimura, A.; Yamashita, T.; Aida, T. Phosphorescent Organogels via “Metallophilic” Interactions for Reversible RGB-Color Switching. *J. Am. Chem. Soc.* **2005**, *127*, 179–183.
39. Kishimura, A.; Yamashita, T.; Yamaguchi, K.; Aida, T. Rewritable phosphorescent paper by the control of competing kinetic and thermodynamic self-assembling events. *Nat. Mater.* **2005**, *4*, 546–549.
40. Mason, W.R. Electronic Structure and Spectra of Linear Dicyano Complexes. *J. Am. Chem. Soc.* **1973**, *95*, 3573–3581.
41. Rawashdeh-Omary, M.A.; Omary, M.A.; Patterson, H.H. Oligomerization of Au(CN)₂⁻ and Ag(CN)₂⁻ Ions in Solution via Ground-State Auophilic and Argentophilic Bonding. *J. Am. Chem. Soc.* **2000**, *122*, 10371–10380.
42. Rawashdeh-Omary, M.A.; Omary, M.A.; Patterson, H.H.; Fackler, J.P., Jr. Excited-State Interactions for [Au(CN)₂⁻]_n and [Ag(CN)₂⁻]_n Oligomers in Solution. Formation of Luminescent Gold-Gold Bonded Excimers and Exciplexes. *J. Am. Chem. Soc.* **2001**, *123*, 11237–11247.

43. Moriuchi, T.; Yoshii, K.; Katano, C.; Hirao, T. Poly-L-lysine-induced Self-association and Luminescence of Dicyanoaurate(I). *Chem. Lett.* **2010**, *39*, 841–843.
44. Pochan, D.J.; Pakstis, L.; Ozbas, B.; Nowak, A.P.; Deming, T.J. SANS and cryo-TEM Study of Self-assembled Diblock Copolypeptide Hydrogels with Rich Nano-through Microscale Morphology. *Macromolecules* **2002**, *35*, 5358–5360.
45. Novak, A.P.; Breedveld, V.; Pakstis, L.; Ozbas, B.; Pine, D.J.; Pochan, D.; Deming, T.J. Rapidly Recovering Hydrogel Scaffolds from Self-assembling Diblock Copolypeptide Amphiphiles. *Nature* **2002**, *417*, 424–428.
46. Deming, T.J. Methodologies for Preparation of Synthetic Block Copolypeptides: Materials with Future Promise in Drug Delivery. *Adv. Drug Deliv. Rev.* **2002**, *54*, 1145–1155.
47. Breedveld, V.; Nowak, A.P.; Sato, J.; Deming, T.J.; Pine, D.J. Rheology of Block Copolypeptide Solutions: Hydrogels with tunable properties. *Macromolecules* **2004**, *37*, 3943–3953.
48. Deming, T.J. Polypeptide Hydrogels via a Unique Assembly Mechanism. *Soft Matter* **2005**, *1*, 28–35.
49. Holowka, E.P.; Sun, V.Z.; Kamei, D.T.; Deming, T.J. Polyarginine Segments in Block Copolypeptides Drive both Vesicular Assembly and Intracellular Delivery. *Nat. Mater.* **2007**, *6*, 52–57.
50. Yang, C.-Y.; Song, B.; Ao, Y.; Nowak, A.P.; Abelowitz, R.B.; Korsak, R.A.; Havton, L.A.; Deming, T.J.; Sofroniew, M.V. Biocompatibility of Amphiphilic Diblock Copolypeptide Hydrogels in the Central Nervous System. *Biomaterials* **2009**, *30*, 2881–2898.
51. Tomczak, M.M.; Glawe, D.D.; Drummy, L.F.; Lawrence, C.G.; Stone, M.O.; Perry, C.C.; Pochan, D.J.; Deming, T.J.; Naik, R.R. Polypeptide-Templated Synthesis of Hexagonal Silica Platelets. *J. Am. Chem. Soc.* **2005**, *127*, 12577–12582.
52. Bellomo, E.G.; Deming, T.J. Monoliths of Aligned Silica-Polypeptide Hexagonal Platelets. *J. Am. Chem. Soc.* **2006**, *128*, 2276–2279.
53. Higuchi T.; Tajima, A.; Yabu, H.; Shimomura, M. Spontaneous Formation of Polymer Nanoparticles with Inner Micro-Phase Separation Structures. *Soft Matter* **2008**, *4*, 1302–1305.
54. Yabu, H.; Koike, K.; Motoyoshi, K.; Higuchi, T.; Shimomura, M. A Novel Route for Fabricating Metal-Polymer Composite Nanoparticles with Phase-Separated Structures. *Macromol. Rapid Commun.* **2010**, *31*, 1267–1271.
55. Camerel, F.; Strauch, P.; Antonietti, M.; Faul, C.F.J. Copper-Metallomesogen Structures Obtained by Ionic Self-Assembly (ISA): Molecular Electromechanical Switching Driven by Cooperativity. *Chem. Eur. J.* **2003**, *9*, 3764–3771.
56. Kuroiwa, K.; Yoshida, M.; Masaoka, S.; Kaneko, K.; Sakai, K.; Kimizuka, N. Self-Assembly of Tubular Microstructures from Mixed-Valence Metal Complexes and Their Reversible Transformation by External Stimuli. *Angew. Chem. Int. Ed.* **2012**, *51*, 656–659.